Journal of Photochemistry and Photobiology A: Chemistry 200 (2008) 402–409

Contents lists available at ScienceDirect

Journal of Photochemistry and Photobiology A: Chemistry

journal homepage: www.elsevier.com/locate/jphotochem

Effects of anionic surfactant SDS on the photophysical properties of two fluorescent molecular sensors

Junhong Qian, Yufang Xu, Xuhong Qian*, Jiaobing Wang, Shenyi Zhang

State Key Laboratory of Bioreactor Engineering and Shanghai Key Laboratory of Chemical Biology, School of Pharmacy, East China University of Science and Technology, Shanghai 200237, China

ARTICLE INFO

Article history:
Received 12 June 2008
Received in revised form 26 August 2008
Accepted 4 September 2008
Available online 17 September 2008

Keywords:
Fluorescent sensor
Micelle
Premicelle
SDS

ABSTRACT

Two fluorescent molecular sensors CS1 and CS2 were designed and synthesized to probe the aggregate behavior of anionic surfactant SDS. CS1 was based on the photo-induced electron transfer (PET) mechanism, while CS2 was founded on the intramolecular charge transfer (ICT) mechanism. The photophysical properties of CS1–2 in anionic surfactant sodium dodecyl sulfate (SDS) solution were studied by fluorescence and UV–vis methods. The experimental results show that significant absorption and emission spectral responses of CS1 were observed with the addition of SDS: the absorbance and fluorescence intensity decreased first and then increased. The plot of fluorescence intensity of CS1 versus SDS concentration showed two break points, which might be ascribed to the critical micellar concentration (cmc) and the formation of premicelle (cac) aggregate, respectively. But the solution's color of CS2 changed from yellow to red with increasing SDS concentrations. The large red-shift in both absorption (50 nm) and emission (55 nm) spectra of CS2 was resulted from the protonation of the electron accepting moiety (N=C nitrogen), which enhanced the "push–pull" interaction of the ICT fluorophore. This was facilitated by the increase of local H^+ concentration around SDS premicelle and micelle. As a consequence, pK_a values of CS1 and CS2 were elevated in SDS micelle.

1. Introduction

Developing fluorescent chemosensors used for detecting the variations in environment or physiological phenomena has been extensively pursued because these sensors can provide real-time, in situ and non-invasive monitoring information with fast response [1–5]. Many fluorescent sensors utilizing the following two distinct design principles: internal charge transfer (ICT) [6–10] and photoinduced electron transfer (PET) [11–13]. These two design principles have different characteristics: the attractiveness of the ICT sensors lies on their two-channel output signals (color change and fluorescence variation), which are convenient and sensitive for the practical utilization; whereas "off-on" or "on-off" fluorescence would occur when a PET sensor binds the guest (Scheme 1).

In the present study, we used a PET sensor CS1 and an ICT sensor CS2 to study the aggregation behavior of anionic surfactant SDS. For CS1, a tertiary amine group (pK_a ~8.0) [14,15] is appended, which should be protonated in neutral aqueous solution, thus making CS1 more like a cationic amphiphilic molecule and facilitating electrostatic attraction with anionic SDS [16–23]. 4-aminonaphthalimide fluorophore is expected to produce an optical signal upon changing its microenvironmental properties when interactions between CS1 and SDS assemblies occur. Much attention should be paid to the structural modification on the electron deficient "imide" moiety of CS2, where the O=C oxygen is displaced by a cyclized imine. This modification is expected to elevate the pK_a of the "imine" moiety, which (N=C nitrogen) will be protonated in the slightly acidic microenvironment around anionic SDS micelle (proton is attracted and concentrated there due to electrostatic interaction [21,22]). Consequently, when CS2 is located in SDS micelle, the protonation at the imine nitrogen will enhance the ICT process and results in a spectral shift to the longer wavelength both in the absorption and emission spectra. The plot of fluorescence intensity of CS1 versus SDS concentration presents two break points corresponding to the cmc and critical aggregate concentration (cac) of SDS, respectively. The plot of fluorescence intensity of CS2 shows a break point corresponding to cmc, but distinct wavelength shifts (~50 nm) in both absorption and emission spectra of CS2 are observed with the addition of SDS. pK_a values of CS1 and CS2 are elevated in SDS micelle due to its "proton-sponge" effect [21,22].

* Corresponding author. Tel.: +86 514 87875805.
E-mail address: xhqian@ecust.edu.cn (X. Qian).

1010-6030/$ – see front matter © 2008 Elsevier B.V. All rights reserved.
doi:10.1016/j.jphotochem.2008.09.002

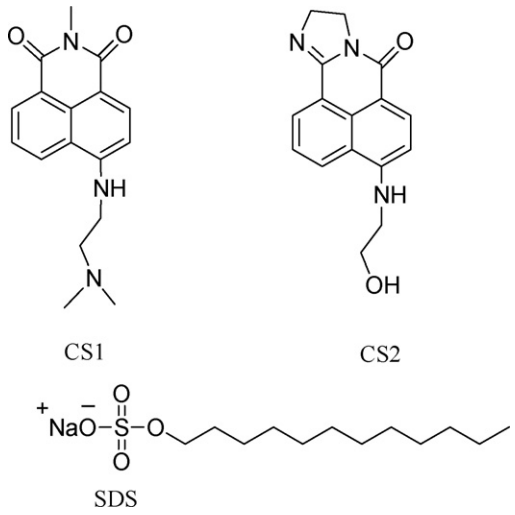

Scheme 1. Molecular structures of CS1, CS2 and SDS.

2. Experimental

2.1. Reagents

All the solvents and reagents were of analytic grade and used as received, Sodium dodecylsulfate (SDS, Sigma, 99%). Water used was twice distilled.

2.2. Absorbance and fluorescence titration

Dye and SDS aqueous solution were prepared with water. Appropriate aliquots of 0.606 M SDS aqueous solution were added to the dye solution followed by stirring and stabilization period before spectral measurements. The pH values were adjusted with 5 M NaOH and HCl aqueous solution and recorded after stable for 1 min. The pH was determined with a pH meter (Shanghai Rex Instrument Factory, China; model PHS-3C), which was standardized with Aldrich buffers. Absorption measurements were performed with a Varian Cary 500 spectrophotometer (1 cm quartz cell) and fluorescence spectra were recorded on a Varian Cary Eclipse fluorescence spectrophotometer (1 cm quartz cell). Mass spectra (MS) were recorded on a MA1212 instrument using standard conditions (ESI, 70 eV). All the experiments were performed at 25.0 ± 0.1 °C.

2.3. Synthesis

The synthesis of CS1–2 from commercially available starting materials is illustrated in Scheme 2.

2.3.1. N-methyl-4-bromonaphthalene-1,8-dicarboximide (*1*)

4-Bromo-1,8-naphthalic anhydride (1.11 g, 4 mmol) was suspended in 33% methyl amine aqueous solution. The mixture was stirred for 10 h at room temperature. The product was obtained by filter and crystallized from ethanol, yield 90%. m.p. 150.3–151.2 °C; 1H NMR (400 MHz, $CDCl_3$): δ8.68–8.65 (d, *J* = 7.5 Hz, 1H), 8.56 (d, *J* = 7.9 Hz, 1H), 8.41 (d, *J* = 7.9 Hz, 1H), 8.04 (d, *J* = 7.8 Hz, 1H), 7.84 (t, *J* = 7.9 Hz, 1H), 3.57 (s, 3H); MS: *m*/*z* (%) 289 (100%).

2.3.2. CS1

0.2 g (0.69 mmol) of **1** and excess N,N-dimethyl ethylenediamine (1 mL) were added to a solution of 5 mL of ethylene glycol monomethyl ether. The mixture was refluxed for 3 h under N_2 atmosphere and then the solvent was evaporated under vacuum. The product was purified by chromatography using methanol/dichloromethane (1:10, v/v) as eluant to give 164 mg (80%) of CS1 as yellow solid. 1H NMR (400 MHz, $CDCl_3$): δ8.68 (d, *J* = 7.6 Hz, 1H), 8.55 (d, *J* = 8.4 Hz, 1H), 8.34 (d, *J* = 8.4 Hz, 1H), 7.74 (t, *J* = 8.0 Hz, 1H), 6.75 (d, *J* = 8.4 Hz, 1H), 6.55 (s, 1H), 3.63 (s, 3H), 3.54 (t, *J* = 4.8 Hz, 2H), 2.92 (t, *J* = 4.4 Hz, 2H), 2.52 (s, 6H). HR-MS (ES^+) Calcd. for $([M+H])^+$, 298.1556; Found, 298.1555.

2.3.3. N-(aminoethyl)-4-bromonaphthalene-1,8-dicarboximide (*2*)

Ethylenediamine (2.0 g, 33.3 mmol) was added to a suspension of 4-bromo-1,8-naphthalic anhydride (5.54 g, 20 mmol) in ethanol (50 mL). The mixture was then refluxed for 4 h, after which the solvent was evaporated under vacuum. The product was crystallized

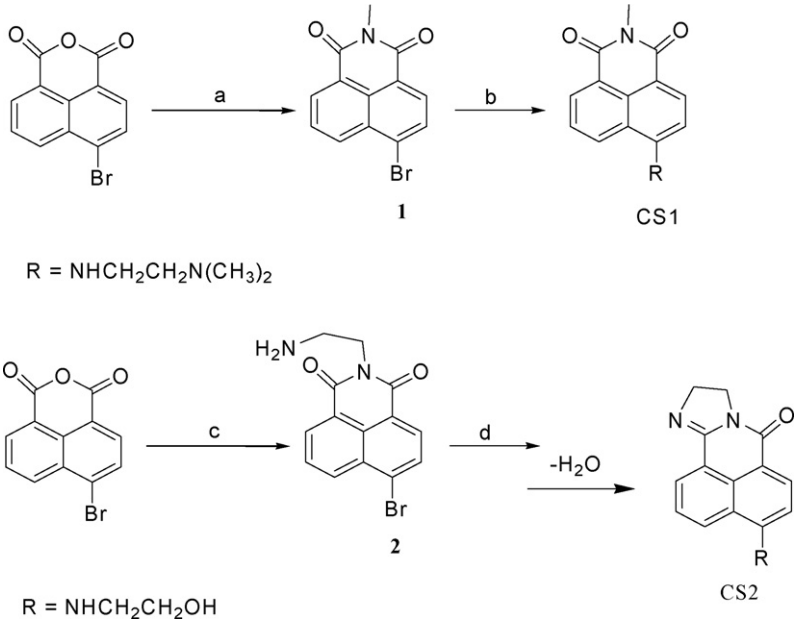

Scheme 2. Preparation of CS1–2. Reagents: (a) 33% methyl amine aqueous solution, (b) N,N-dimethyl ethylenediamine, ethylene glycol monomethyl ether; (c) ethylenediamine, EtOH; (d) ethanolamine, ethylene glycol monomethyl ether.

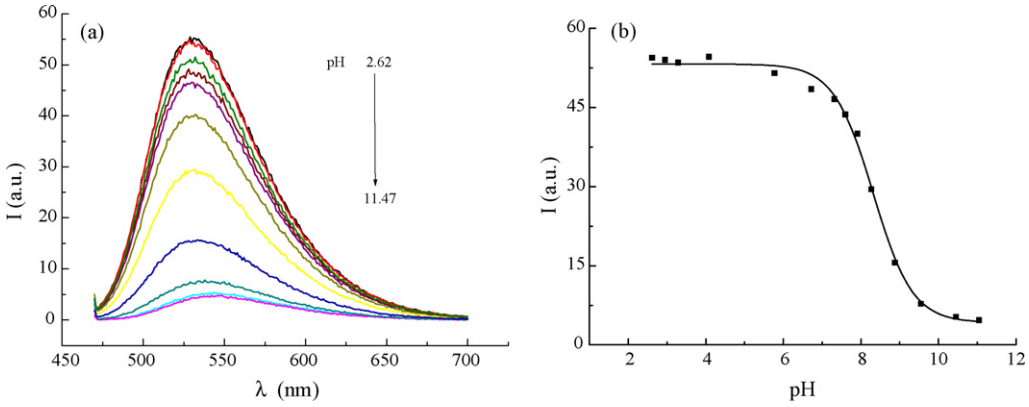

Fig. 1. pH effect on the emission spectra of CS1 (a) and the plot of fluorescence intensity vs. solution's pH (b) ([CS1] = 2.8×10^{-6} M, λ_{ex} = 465 nm).

from ethanol and obtained as slight yellow solid, yield 85%. 1H NMR (500 MHz, $CDCl_3$): δ8.65 (dd, 1H), 8.56 (dd, 1H), 8.41 (d, *J* = 7.9 Hz, 1H), 8.04 (d, *J* = 7.8 Hz, 1H), 7.85 (dd, 1H), 4.27 (t, *J* = 6.6 Hz, 2H), 3.07 (t, *J* = 6.6 Hz, 2H), 1.04 (s, 2H); MS: *m/z* (%) 318 (1%).

2.3.4. CS2

0.2 g (0.63 mmol) of **2** and excess ethanol amine (1 mL) were added to a solution of 5 mL of ethylene glycol monomethyl ether. The mixture was refluxed for 5 h under N_2 atmosphere and then the solvent was evaporated under vacuum. The product was purified by chromatography using methanol/dichloromethane (1:10, v/v) as eluant to give 40 mg (20%) of CS2 as yellow solid. 1H NMR (400 MHz, CD_3OD): δ8.35 (d, *J* = 7.3 Hz, 1H), 8.30 (d, *J* = 7.2 Hz, 1H), 8.16 (d, *J* = 7.5 Hz, 1H), 7.55 (t, *J* = 7.8 Hz, H), 6.74 (d, *J* = 7.9 Hz, 1H), 4.18–4.05 (m, *J* = 6.3 Hz, 4 H), 3.87 (t, *J* = 6.3 Hz, 2 H), 3.56 (t, *J* = 6.1 Hz, 2H). HR-MS (ES+) Calcd. for $([M+H])^+$, 282.1243; Found, 282.1249.

3. Results

3.1. pH effect on the absorption and emission spectra of CS1

When pH was changed from 2.62 to 11.47, the absorbance of CS1 had no obvious change, but its absorption maximum shifted slightly to longer wavelength (+11 nm) at basic pH range (data are not shown). The fluorescence intensity of CS1 decreased steadily without noticeable wavelength shift. Fig. 1b shows that when pH changes from 6 to 9, the fluorescence intensity decreases sharply. The deprotonation of appended quaternary amine salt initiates the PET process from the free tertiary amine to the excited fluorophore. As a result, the fluorescence intensity decreases rapidly. The pK_a value of CS1 obtained from Fig. 1b is 8.52. In the acidic region (pH < 4), the fluorescence intensity of CS1 has no evident change, which may suggest

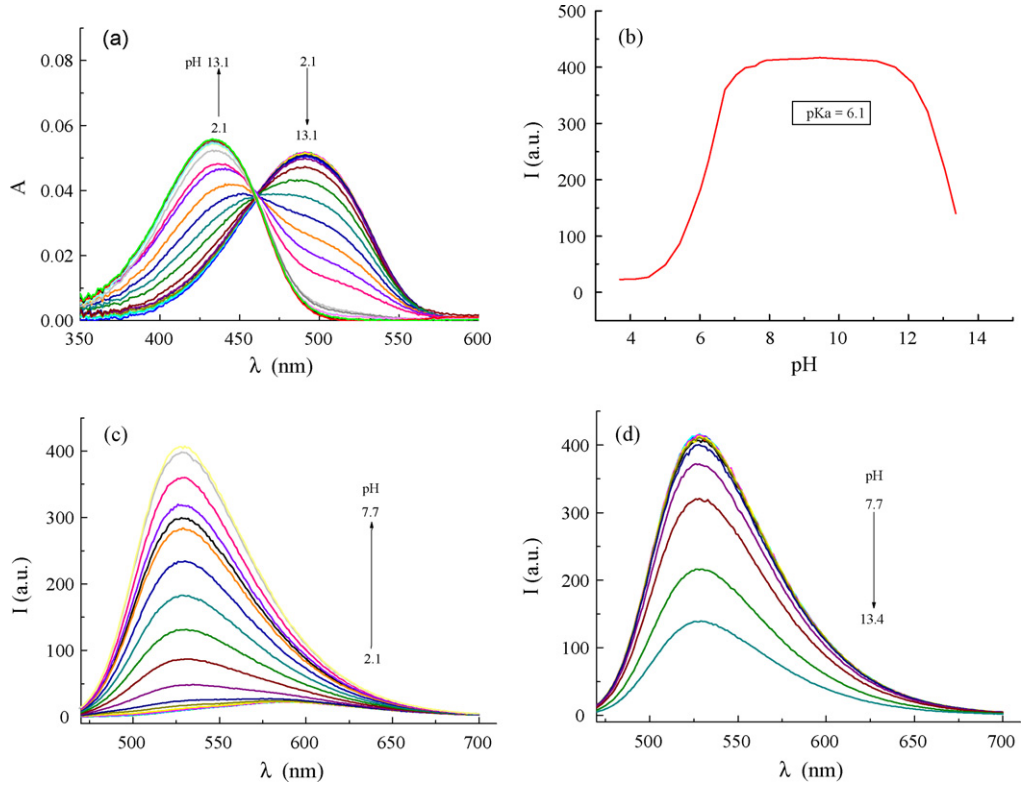

Fig. 2. pH effect on the absorption (a), emission (c and d) spectra of CS2 and the plot of fluorescence intensity vs. solution's pH (b) ([CS2] = 3.2×10^{-6} M, λ_{ex} = 465 nm).

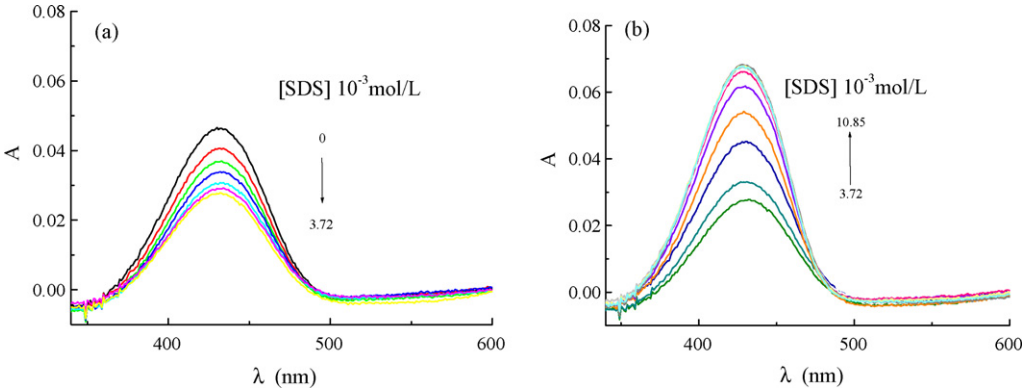

Fig. 3. SDS effects on the absorption spectra of CS1 ([CS1] = 2.8×10^{-6} M).

that the appended tertiary amine is totally protonated in this region.

3.2. pH effect on the absorption and emission spectra of CS2

The absorption and emission spectra of CS2 in neutral aqueous solution display a maximum at 446 and 528 nm, respectively, which are assigned to the ICT process from the electron donor moiety (the amine nitrogen atom) to the electron deficient moiety (imine in dihydroimidazole heterocycle). Addition of hydrochloric acid to CS2 in aqueous solution shows a color change which is perceptible to the naked eye, from yellow to red. The dependence of absorbance on pH are found to show a significant decrease in 446 nm and increase in a new longer absorption band (496 nm, Fig. 2a), the protonation of imine (C=N) nitrogen enhanced the "push–pull" character of the ICT transition, which caused a considerable hyperchromic shift (+50 nm) in absorbance spectra, and an isosbestic point at 465 nm is clearly seen.

The fluorescence intensity of CS2 in aqueous solution was significantly quenched in 528 nm upon addition of aqueous hydrochloric acid (from pH 7.7 to 2.1, Fig. 2c), and a very weak red-shift emission (λ_{max} = 583 nm) was observed. This spectra change was caused by the protonation process of the imine (C=N) nitrogen which opened up the non-radiative deexcitation pathway[3a] such as solvent effect of water. The addition of NaOH (from pH 7.7 to 13.4, Fig. 2d) to the neutral aqueous solution, initiated another fluorescence quenching pathway, e.g. the decyclization of naphthalene-1,8-dicarboximide cycle induced the molecular vibration. As a whole, a bell-shaped pH titration curve reflecting the "off-on-off" fluorescence response was achieved. The pK_a value of CS2 (6.08) obtained from Fig. 2b elucidates that the imine (C=N) nitrogen may be protonated in a pH range close to physiologically relevant range.

3.3. SDS effects on the UV–vis and fluorescence spectra of CS1

SDS titration induced dramatic spectral changes in both the absorption and fluorescence spectra of CS1 (Figs. 3 and 4). When SDS was increased from 0 to 3.72 mM (well below the cmc of SDS), the absorbance at 432 nm was decreased monotonously from $\varepsilon = 1.67 \times 10^4$ to 1.02×10^4 M^{-1} cm^{-1} without notable wavelength shift. Above this, it was increased steadily ($\varepsilon = 2.48 \times 10^4$ M^{-1} cm^{-1} at SDS = 7.82×10^{-3} M) with a slight blue-shift (~5 nm). Similar trends in the emission spectra were also observed (Fig. 4). Fluorescence quantum yields ϕ in the presence of 0, 4.52, and 7.82 mM SDS were 0.181, 0.120, and 0.322, respectively [24].

Two break points are clearly observed in the titration curve of CS1 (absorption, Fig. 5a): the one at 6.9×10^{-3} M is corresponding to the cmc of SDS [25,37], the other at 3.7 mM is attributed to the formation of SDS premicelle [37]. Similar titration curve is observed in the emission spectra (Fig. 5b), where the two break points are found at 6.9 and 4.3 mM, respectively.

3.4. SDS effects on the UV–vis and fluorescence spectra of CS2

As for sensor CS2, SDS titration induced spectral responses different from that of CS1. No distinct spectral changes were observed until SDS was added up to 4.85 mM (Figs. 6 and 7). Beyond this, a

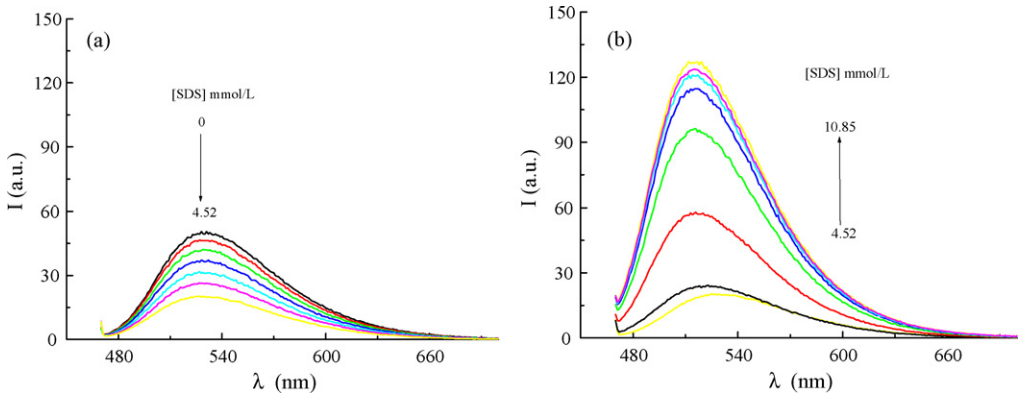

Fig. 4. SDS effects on the emission spectra of CS1 ([CS1] = 2.8×10^{-6} M, λ_{ex} = 465 nm).

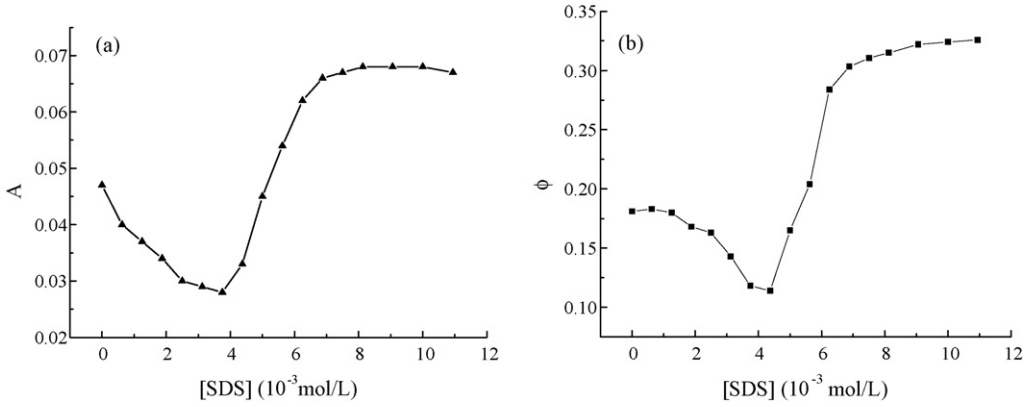

Fig. 5. Plots of absorbance at 432 nm (a) and quantum yield ϕ (b) of CS1 vs. C_{SDS} ([CS1] = 2.8×10^{-6} M, λ_{ex} = 465 nm).

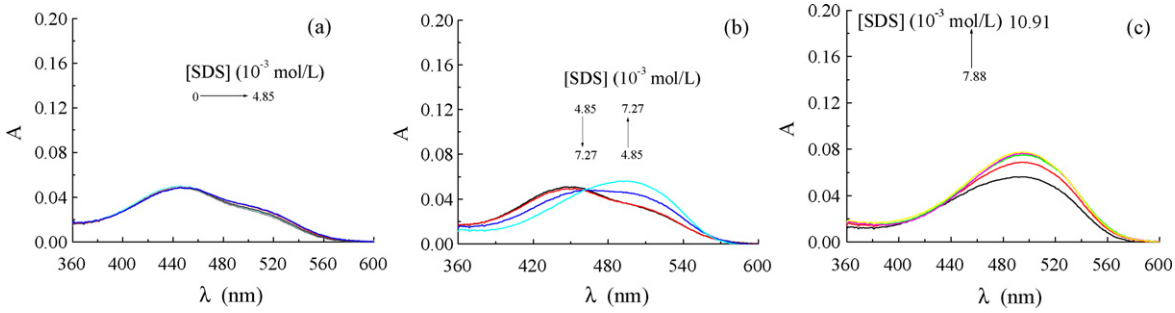

Fig. 6. SDS effects on the absorption spectra of CS2 ([CS2] = 3.2×10^{-6} M).

new absorption band centered at 496 nm was formed and developed at the expense of the original band centered at 446 nm, yielding an isosbestic point at 465 nm (Fig. 6b). When SDS was increased from 4.85 to 7.88 mM, a new emission band at longer wavelength (583 nm) was produced, which coexisted with the original one (528 nm) but possessing decreased intensity. This spectral change was consistent with the red-shift observed in the absorption spectra. Further addition of SDS did not produce dramatic spectral changes.

3.5. Effect of SDS on the pK_a values of CS1 and CS2

Fig. 8a shows the change of fluorescence intensities with pH in 11 mM SDS micelle, from which we can obtain the pK_a values of CS1 and CS2 in SDS micelle are 10.10 and 8.17, respectively. But those in water are 8.52 and 6.08, respectively. The higher pK_a values in SDS micelle reveal that CS1 and CS2 are located in SDS micelles. This result also proves the "proton sponge effect" of SDS on the other hand. From the pK_a value vs. SDS concentration plots (Fig. 8b), we can know that the pK_a values of both CS1 and CS2 increase with SDS concentration at [SDS] less than 8 mM, above this they hardly have any change, which may indicate that CS1 and CS2 are almost completely incorporated into SDS micelles at [SDS] above 8 mM.

4. Discussions

The optical responses of CS1–2 upon SDS addition are summarized in Table 1. For CS1, the absorbance and fluorescence intensity were decreased remarkably without any wavelength shift in the presence of 4.24 mM SDS. Upon SDS addition up to 7.88 mM, they were recovered and larger than the initial values with slightly blue shift in both absorption and emission spectra. For CS2, the absorption and fluorescence spectra remained unaffected until SDS was added up to 4.8 mM. The absorbance was increased while fluorescence quantum yield was decreased with significantly red shift in both absorption and emission spectra in SDS micelle, which led to the color's change (Table 1).

The two channel optical responses of CS1 upon SDS addition are related to the structure character of CS1 as well as the microenvironmental factors, such as the polarity and "H^+ sponge effect"

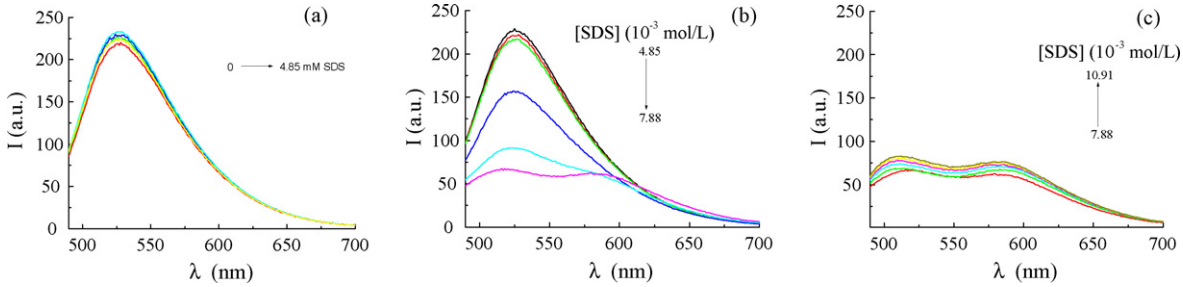

Fig. 7. SDS effects on the emission spectra of CS2 ([CS2] = 3.2×10^{-6} M, λ_{ex} = 465 nm).

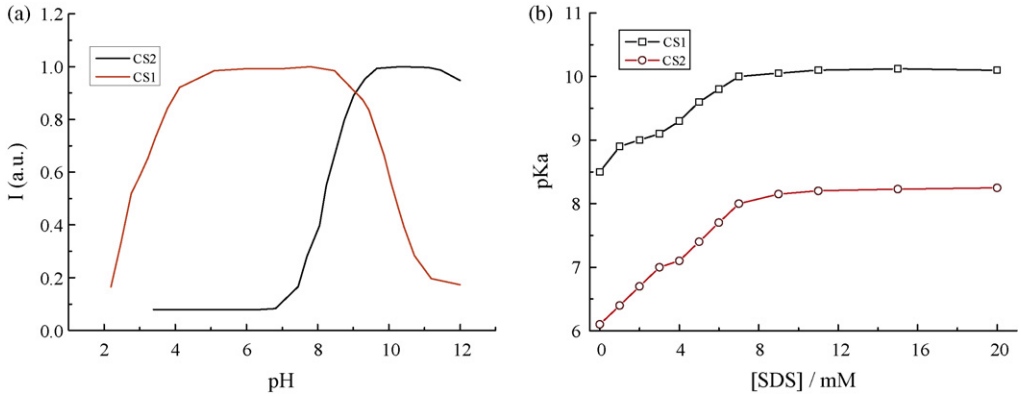

Fig. 8. Plots of normalized fluorescence intensities (a) of CS1 and CS2 vs. pH in 11 mM SDS micelle and the pK_a plots (b) of CS1 and CS2 vs. SDS concentrations.

Table 1
Spectral data for CS1–2 at different SDS concentrations.

C_{SDS} (mM)	CS1				CS2			
	λ_{abs} (nm)	ε (10^4 M^{-1} cm^{-1})	λ_{fl} (nm)	ϕ	λ_{abs} (nm)	ε (10^4 M^{-1} cm^{-1})	λ_{fl} (nm)	ϕ
0	432	1.67	530	0.181	446	1.58	528	0.060
4.24	432	1.12	530	0.128	446	1.59	528	0.063
7.88	428	2.49	515	0.323	496	1.73	583	0.025

of anionic SDS premicelle and micelle [21,22]. CS1, equipped with a tertiary amine, which has a pK_a of 8.52 (Scheme 3), was protonated in the present experimental conditions (pH 6.40 ± 0.10). With the addition of SDS, the positively charged CS1 will undergo the following three processes due to the electrostatic attraction: forming aggregates $(CS2)_m(SDS)_n$ with SDS, dissolving in SDS premicelle and penetrating into SDS micelle. In the presence of small amount of SDS (less than the 1 mM), CS1 can form soluble aggregates with SDS, which decreases the absorbance at 432 nm. The fluorophores, buried in the soluble aggregates, are largely quenched because of their proximity which facilitates electron and energy transfer. Therefore, the emission intensity is quenched significantly. With further addition of SDS, the aggregates become larger, some aggregates are insoluble in water due to the decreased overall charge density, which results in the decrease of the absorbance and fluorescence intensity [16–23]. The insoluble aggregates couldn't make the fluorescence quantum yield ϕ be changed evidently. But the ϕ value of CS1 was decreased gradually when SDS concentration was less than 4.24 mM (Fig. 5b), which suggested that there coexisted soluble aggregates at c_{SDS} in the range of 1–4.24 mM [37].

When SDS concentrations are in the range of cac∼cmc, the hydrophobic interaction and the electrostatic attraction between SDS and CS1 make $(CS1)_m(SDS)_n$ aggregates reorganize into premicelles with a monomeric CS1 molecule. As a consequence, the microenvironmental polarity surrounding CS1 molecules is depressed, and the fluorescence quenching pathways, such as enhanced hydrogen bond with water molecule in the excited state, are suppressed. Meanwhile, because $C_{SDS} \gg C_{CS1}$, [26,27] it is difficult for two sensor molecules to locate in the same premicelle. Thus, collision induced fluorescence quenched is hampered, which results in an enhanced fluorescence (Fig. 4b). The increase of the absorbance (Fig. 3b) is resulted from the decomplexation of the aggregates $(CS2)_m(SDS)_n$. With further increase of SDS above its cmc, the absorbance and fluorescence intensity reaches the limiting value and all dye molecules are incorporated into normal micelles in monomeric form. In addition, SDS micelle provides a less polar environment for CS1 molecules, which leads to a blue shift in absorption (4 nm, Table 1) and emission (15 nm, Table 1) maxima [28]. The almost twice enhancement in ϕ value of CS1 (from 0.181 in water to 0.323 in SDS micelle, Table 1) is benefited from the less polar micelle and the higher H^+ concentration around SDS micelle. It should be mentioned that carbonyl oxygen in CS1 couldn't be protonated in SDS micelle due to its lower pK_a (<2.0) [29]. So, its absorption and emission maxima had no obvious change with the addition of SDS up to 4.24 mM (Table 1).

CS2 is a nonionic compound in the neutral aqueous solution (Scheme 3). So, no electrostatic attraction between CS2 and SDS is present. When SDS concentrations are lower than its cac, it

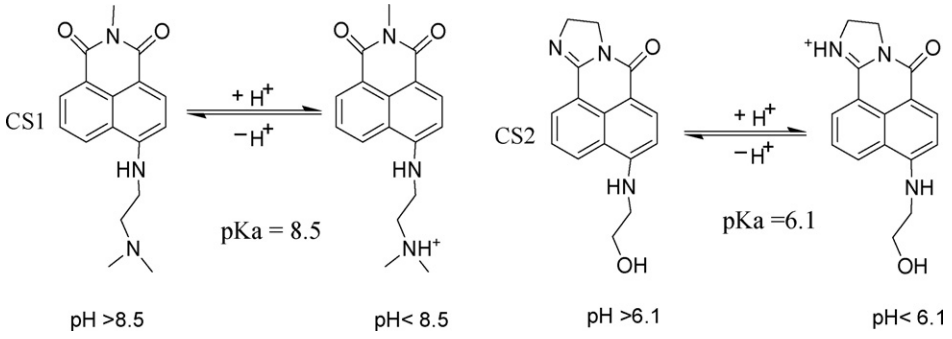

Scheme 3. Protonation process of CS1 and CS2.

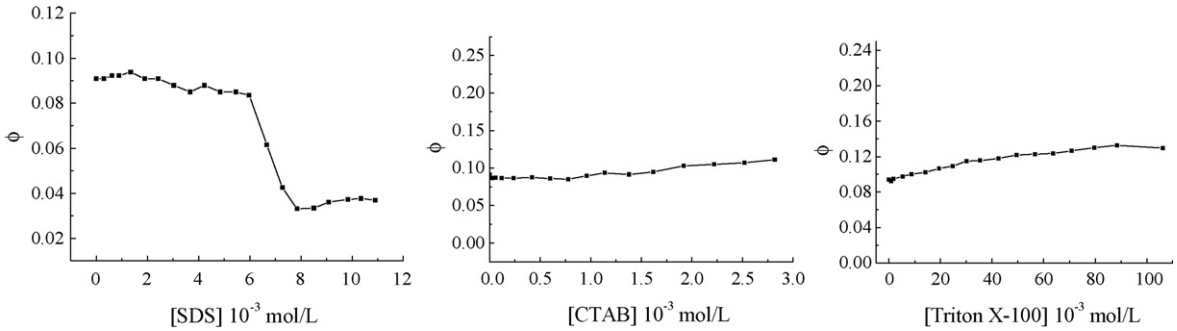

Fig. 9. Effects of CTAB and Triton X-100 on the UV–vis and fluorescence spectra of CS2 (pH 6.40–6.50 for Triton X-100 system, pH 6.30 ± 0.10 for CTAB system).

is dissolved in water as monomer and has no evident effect on the spectral behavior of CS2. When SDS concentrations are in the premicellar range (4.85–7.88 mM), CS2 molecules are located in premicelles ascribed to the hydrophobic interaction between SDS and CS2.

The higher H^+ concentration adsorbed on SDS micellar surface makes CS2 be protonated to form monoprotonic species [30,31] (its pK_a 8.17 in SDS micelle, Fig. 8), which results in an increase in absorbance at 496 nm (Fig. 6b) as well as decreases in the emission at 528 nm (Fig. 7b) and the ϕ value of CS2 (Table 1). Moreover, when SDS concentration is larger than its cmc, the microenvironmental polarity surrounding CS2 is decreased. The ICT process is depressed to some extent, which results in a slight enhancement in absorbance and fluorescence intensity. The increase in the cationic emission of CS2 in the micellar environment implies that the species does not penetrate into the micellar core but rather sites closer to the micellar surface where it is electrostatically stabilized.

In order to verify the importance of the electrostatic attraction in the detection of surfactant aggregates, we also studied the effects of cationic surfactant CTAB and nonionic surfactant Triton X-100 on the UV–vis and fluorescence spectra of CS1 and CS2.

CTAB and Triton X-100 hardly affect the spectral properties of CS1, because electrostatic repulsion exists between cationic species of CS1 and CTAB (or Triton X-100 due to its partly cationic properties) [32]. The absorption spectrum of CS2 has no visible change upon the addition of CTAB and Triton X-100, while its fluorescence intensity increases slightly with increasing CTAB and Triton X-100 concentrations (Fig. 9). But no distinct break point is observed in Fig. 9. These results indicate that the hydrophobic interaction between CTAB (or Triton X-100) and CS2 is not strong enough to bring CS2 into CTAB or Triton X-100 micelles. As a consequence, CTAB and Triton X-100 have little influence on the spectral behavior of CS2. The almost unchanged absorption and emission spectra in CTAB and Triton X-100 micelles suggests that CS2 may locate at the interface of SDS micelle. It also reveals that the electrostatic attraction plays an important role in the detection of surfactant aggregates.

5. Conclusions

Both fluorescent sensors CS1–2 can be used to detect the self-assembly aggregation behavior of SDS. CS1 showed dual optical response of premicelle and micelle ascribed to cationic nature in neutral water solution. For CS2, a 50 nm red-shift in absorption spectra upon addition of SDS led to the change in solution's color, which made the detection of self-assembly aggregations more convenient. The electrostatic attraction plays a main role in the detection of aggregate behavior, and the change of ICT process with microenvironment is important for guest-detecting with color change. The pK_a values of CS1 and CS2 were elevated in SDS micelle. CS1 and CS2 provide a new strategy to probe the structural transformation of the self-assembly aggregates, which is different from the transformation of pyrene between the excimer and the monomer [33–37].

Acknowledgements

This work was financially supported by the National Natural Science Foundation of China (20536010), the National Key Project for Basic Research (2003CB 114400) and the Science and Technology Foundation of Shanghai.

References

[1] H. He, M.A. Mortellaro, M.J.P. Leiner, S.T. Young, R.J. Fraatz, J.K. Tusa, A fluorescent chemosensor for sodium based on photoinduced electron transfer, Anal. Chem. 75 (2003) 549–555.
[2] S. Uchiyama, Y. Matsumura, A.P. de Silva, K. Iwai, Modulation of the sensitive temperature range of fluorescent molecular thermometers based on thermoresponsive polymers, Anal. Chem. 76 (2004) 1793–1798.
[3] M. Licchelli, A.O. Biroli, A. Poggi, A prototype for the chemosensing of Ba^{2+} based on self-assembling fluorescence enhancement, Org. Lett. 8 (2006) 915–918.
[4] N.A. O'Connor, S.T. Sakata, H. Zhu, K.J. Shea, Chemically modified dansyl probes: s fluorescent diagnostic for ion and proton detection in solution and in polymers, Org. Lett. 8 (2006) 1581–1584.
[5] O. van den Berg, W.F. Jager, S.J. Picken, 7-Dialkylamino-1-alkylquinolinium salts: highly versatile and stable fluorescent probes, J. Org. Chem. 71 (2006) 2666–2676.
[6] T. Yoshihara, S.I. Druzhinin, K.A. Zachariasse, Fast intramolecular charge transfer with a planar rigidized electron donor/acceptor molecule, J. Am. Chem. Soc. 126 (2004) 8535–8539.
[7] J. Seo, S. Kim, S.Y. Park, Strong solvatochromic fluorescence from the intramolecular charge-transfer state created by excited-state intramolecular proton transfer, J. Am. Chem. Soc. 126 (2004) 11154–11155.
[8] Z. Xu, X. Qian, J. Cui, Colorimetric and ratiometric fluorescent chemosensor with a large red-shift in emission: Cu(II)-only sensing by deprotonation of secondary amines as receptor conjugated to naphthalimide fluorophore, Org. Lett. 7 (2005) 3029–3032.
[9] B. Liu, H. Tian, A ratiometric fluorescent chemosensor for fluoride ions based on a proton transfer signaling mechanism, J. Mater. Chem. 15 (2005) 2681–2686.
[10] J. Wang, X. Qian, J. Cui, Detecting Hg^{2+} ions with an ICT fluorescent sensor molecule: remarkable emission spectra shift and unique selectivity, J. Org. Chem. 71 (2006) 4308–4311.
[11] J.F. Callan, A.P. de Silva, J. Ferguson, A.J.M. Huxley, A.M. O'Brien, Fluorescent photoionic devices with two receptors and two switching mechanisms: applications to pH sensors and implications for metal ion detection, Tetrahedron 60 (2004) 11125–11131.
[12] V. Thiagarajan, P. Ramamurthy, D. Thirumalai, V.T. Ramakrishnan, A novel colorimetric and fluorescent chemosensor for anions involving PET and ICT pathways, Org. Lett. 7 (2005) 657–660.
[13] A. Coskun, E. Deniz, E.U. Akkaya, Effective PET and ICT switching of boradiazaindacene emission: a unimolecular, emission-mode, molecular half-subtractor with reconfigurable logic gates, Org. Lett. 7 (2005) 5187–5189.
[14] A.P. de Silva, H.Q.N. Gunaratne, P.L.M. Lynch, A.J. Patty, G.L. Spence, Luminescence and charge transfer. part 3. the use of chromophores with ICT (internal charge transfer) excited states in the construction of fluorescent PET (photoinduced electron transfer) pH sensors and related absorption pH sSensors with aminoalkyl side chains, J. Chem. Soc. Perkin Trans. 2 (1993) 1611–1616.
[15] A.P. de Silva, H.Q.N. Gunaratne, J. Habib-Jiwan, C.P. McCoy, T.E. Rice, J. Soumillion, Study of photoinduced electron transfer: the influence of a molecular

electric field in the excited state, Angew. Chem. Int. Ed. Engl. 34 (1995) 1728–1731, pKa values in their exited (S1) state for CS1–2 were measured according following equation: $\log[(\phi_{max} - \phi)/(\phi - \phi_{min})] = pH - pK_a$.
[16] H. Sato, M. Kawasaki, K. Kasatani, Fluorescence and energy transfer of dye-detergent system in the premicellar region, J. Photochem. 17 (1981) 243–248.
[17] M. Deumié, M.E. Baraka, Self-aggregation of R110 and R123 rhodamines with surfactants and phospholipid vesicles of negative charge: a qualitative fluorescence study, J. Photochem. Photobiol. A 74 (1993) 255–266.
[18] P. Bilski, R.N. Holt, C.F. Chignell, Premicellar aggregates of rose bengal with cationic and zwitterionic surfactants, J. Photochem. Photobiol. A 110 (1997) 67–74.
[19] A. Mishra, R.K. Behera, B.J. Mishra, G.B. Behera, Dye-surfactant interaction: chain folding during solubilization of styryl pyridinium dyes in sodium dodecyl sulfate aggregates, J. Photochem. Photobiol. A 121 (1999) 63–73.
[20] R.V. Pereira, M.H. Gehlen, Fluorescence of acridinic dyes in anionic surfactant solution, Spectrochim. Acta A 61 (2005) 2926–2932.
[21] A. Chakrabarty, A. Mallick, B. Haldar, P. Purkayastha, P. Das, N. Chattopadhyay, Surfactant chainlength dependent modulation of prototropic transformation of a biological photosensitizer: norharmane in anionic micelles, Langmuir 23 (2007) 4842–4848.
[22] M. Khamis, B. Bulos, F. Jumean, A. Manassra, M. Dakiky, Azo dyes interactions with surfactants. Determination of the critical micelle concentration from acid–base equilibrium, Dyes Pigments 66 (2005) 179.
[23] N.O. Mchedlov-Petrossyan, N.A. Vodolazkaya, O.N. Bezkrovnaya, A.G. Yakubovskaya, A.V. Tolmachev, A.V. Grigorovich, Fluorescent dye *N*,*N*′-dioctadecylrhodamine as a new interfacial acid–base indicator, Spectrochim. Acta A 69 (2008) 1125–1129.
[24] Fluorescence quantum yield $\phi_S = \phi_R[F_S \cdot A_R/(F_R \cdot A_S)]$, subscript S and R represent the sample and reference, respectively; ϕ, F and A are the fluorescence quantum yield, the integral of emission band and absorbance at excited wavelength, respectively.
[25] The cmc of SDS at 25 °C in the literature is in the range of 7.2–8.1 mM. (a) A. Yamagishi, Transient electric dichroism studies on interaction of a cationic dye with sodium dodecylsulfate, J. Colloid Interface Sci. 81 (1981) 511–518.
[26] The aggregation number of SDS is about 60–80, so SDS micelle concentration was about 10^{-4} M, and the concentrations of CS1–2 used in this paper were in the range of $(2.8–3.7) \times 10^{-6}$ M.
[27] R. Karmakar, A. Samanta, Phase-transfer catalyst-induced changes in the absorption and fluorescence behavior of some electron donor-acceptor molecules, J. Am. Chem. Soc. 123 (2001) 3809–3817.
[28] S. Saha, A. Samanta, Influence of the structure of the amino group and polarity of the medium on the photophysical behavior of 4-amino-1,8-naphthalimide derivatives, J. Phys. Chem. A 106 (2002) 4763–4771.
[29] The absorption and fluorescence spectra had no noticeable change in the pH range of 6.0–2.0, which reveals that the pK_a of carbonyl oxygen is smaller than 2.0.
[30] G. Krishnamoorthy, S.K. Dogra, Spectral characteristics of the various prototropic species of 2-(4′-*N*,*N*-dimethylaminophenyl)pyrido[3,4-*d*]imidazole, J. Org. Chem. 64 (1999) 6566–6574.
[31] G. Krishnamoorthy, S.K. Dogra, Twisted intramolecular charge transfer of 2-(4′-*N*,*N*-dimethylaminophenyl)pyrido[3,4-d]imidazole in cyclodextrins: effect of pH, J. Phys. Chem. A 104 (2000) 2542–2551.
[32] G. Zhao, B. Zhu, Principles of Surfactant Action, first ed., Light Industry Press of China, Beijing, 2003.
[33] S.S. Atik, L.A. Singer, Spectroscopic studies on small aggregates of amphipathic molecules in aqueous solution, J. Am. Chem. Soc. 101 (1979) 6759–6761.
[34] M.E.C.D.R. Oliverira, L.C. Pereira, E.W. Thomas, R.H. Bisby, R.B. Cundall, Photochemistry of pyrenylmethyltriphenyl-phosphonium salts and related compounds, J. Photochem. 31 (1985) 373–379.
[35] S.G. Bertolotti, O.E. Zimmerman, J.J. Cosa, C.M. Previtali, Excimer emission of pyrene derivatives induced by ionic detergents below the critical micelle concentration, J. Lumin. 55 (1993) 105–113.
[36] M.E.C.D.R. Oliverira, J.A. Ferreira, S.M. Nascimento, Oligomerization of cationic pyrene derivatives in the presence of sodium dodecyl sulfate: a route to nanoaggregate formation, J. Chem. Soc. Faraday Trans. 91 (1995) 3913–3917.
[37] S.K. Ghosh, A. Pal, S. Kundu, M. Mandal, S. Nath, T. Pal, Emission behavior of 1-methylaminopyrene in aqueous solution of anionic surfactants, Langmuir 20 (2004) 5209–5213.